Direct Measurements of Reynolds Stresses and Turbulence in the Bottom Boundary Layer

Joseph Katz
Department of Mechanical Engineering
The Johns Hopkins University, 3400 N. Charles Street
Baltimore, MD 21218
phone: (410) 516-5470 fax: (410) 516-7254 email: katz@titan.me.jhu.edu

Thomas Osborn
Department of Earth and Planetary Sciences
The Johns Hopkins University
3400 N Charles Street
Baltimore, MD 21218-2681
phone (410) 516-7039 fax (410) 516-7933 email osborn@jhu.edu

Award Number: N000149510215

LONG-TERM GOALS

Predictions of the ocean dynamics, sediment transport, pollutant dispersal and biological processes require knowledge on the characteristics of turbulence in the bottom boundary layer. Our goal is to:

a. Measure the Reynolds stresses (free of wave contamination), velocity profile, dissipation rate, and turbulent spectra in the coastal bottom boundary layer using Particle Image Velocimetry (PIV).

b. Quantify the temporal variation of turbulent stresses, production, dissipation and buoyancy flux in relation to the local oceanographic parameters, such as waves, currents, stratification, internal waves and the nature of the water-sediment interface.

c. Examine the structure of the flow, vertical vorticity transport, formation and upward migrations of large coherent vortex structures. Presently there is very little information on the dynamics and impact of large coherent structure in the bottom boundary layer on turbulence and sediment entrainment.

d. Study the mechanisms and extent of sediment re-suspension process by simultaneously measuring the flow structure and particle distributions.

e. Use the PIV data for addressing Sub-Grid Scale Modeling issues for Large Eddy Simulation in oceanic flows.

OBJECTIVES

During FY03 our effort has focused on the following two major objectives:

a. Perform a series of flow and turbulence measurements in the bottom boundary layer of the Southeastern continental shelf, in the vicinity of the South Atlantic Bight Synoptic Offshore Observational Network (SABSOON). This site provides a wide range of flow conditions within a tidal cycle with peak velocity that significantly exceeds the conditions in previous test sites (LEO-15).

Report Documentation Page

Form Approved
OMB No. 0704-0188

1. REPORT DATE **30 SEP 2003**	2. REPORT TYPE	3. DATES COVERED **00-00-2003 to 00-00-2003**

4. TITLE AND SUBTITLE **Direct Measurements of Reynolds Stresses and Turbulence in the Bottom Boundary Layer**	5a. CONTRACT NUMBER 5b. GRANT NUMBER 5c. PROGRAM ELEMENT NUMBER
6. AUTHOR(S)	5d. PROJECT NUMBER 5e. TASK NUMBER 5f. WORK UNIT NUMBER
7. PERFORMING ORGANIZATION NAME(S) AND ADDRESS(ES) **Department of Mechanical Engineering,,The Johns Hopkins University, 3400 N. Charles Street,,Baltimore,,MD, 21218**	8. PERFORMING ORGANIZATION REPORT NUMBER
9. SPONSORING/MONITORING AGENCY NAME(S) AND ADDRESS(ES)	10. SPONSOR/MONITOR’S ACRONYM(S) 11. SPONSOR/MONITOR’S REPORT NUMBER(S)

12. DISTRIBUTION/AVAILABILITY STATEMENT
Approved for public release; distribution unlimited

13. SUPPLEMENTARY NOTES

14. ABSTRACT

15. SUBJECT TERMS

16. SECURITY CLASSIFICATION OF:			17. LIMITATION OF ABSTRACT	18. NUMBER OF PAGES	19a. NAME OF RESPONSIBLE PERSON
a. REPORT **unclassified**	b. ABSTRACT **unclassified**	c. THIS PAGE **unclassified**	**Same as Report (SAR)**	**9**	

Standard Form 298 (Rev. 8-98)
Prescribed by ANSI Std Z39-18

b. Continuing the analysis of data obtained during previous field trips (funded in part by ONR in part by NSF) to the vicinity of LEO–15 and in the mouth of the Delaware Bay during summer 2000 and Fall 2001. In addition to previously reported results, during this year we have performed:

1. Following previous observations that the turbulence within the bottom boundary layer consists of powerful gusts followed by quiescent periods, we have performed conditional sampling of turbulence statistics, including stresses, dissipation and spectra in periods of high gust and in quiescent periods. As will be demonstrated, all the shear stresses are generated during the high gust periods.

2. Careful examination of the velocity distributions in an attempt to explain the substantial anisotropy of the bottom boundary layer turbulence, as demonstrated in the previous report.

3. Conditional sampling of turbulence statistics based on phase within the wave cycle to determine whether the waves directly affect the turbulence parameters.

4. Analysis sub-grid stress dynamics for Large Eddy Simulations, focusing on dynamic subgrid stress models.

5. Analysis of size and spatial distributions as well as shape of suspended particles within the bottom boundary layer as a function of elevation, mean flow, turbulence intensity and stratification. The PIV images provide information on the total number of particles within the sample area, but not on the shape and size of particles. Thus, we have also utilized video-microscopy to sample a sub-section of the sample area. Automated methods to extract the spatial distributions of particles form the PIV images have been developed. Data analysis is presently in progress.

Since size limitations prevents us from providing details on all the issues mentioned here, we opt to focus only on some topics. The results below summarize the recent field tests, and highlight the structure of near wall turbulence, including the effects of gusts, and the origin of the anisotropy.

APPROACH

PIV measures the instantaneous distributions of two velocity components in a sample area by recording multiple exposure images of particles located within a laser sheet, and measuring their displacement. The oceanic PIV system has been described in previous reports and in refs. 2 - 6. It has two 35x35 cm sample areas and images are acquired using two 2k x 2k CCD cameras, each with a maximum sampling rate of 4 frames/s. A high-speed data acquisition system enables continuous image acquisition for hours. The laser is located on the ship and the light is transmitted through optical fibers to submerged probes. Each camera and associated light sheet can be aligned independently. Each instantaneous velocity distribution consists of 63x63 vectors. Samples are presented in Figure 2.
The submersible components of the PIV system are mounted on a seabed platform deployed from a ship, which can be rotated to align the sample areas with the mean flow direction, and extend vertically to sample at different elevations. The adjustable platform consists of a 5-stage telescopic hydraulic cylinder, with a vertical range of 9.75m. The elevation and orientation are remotely controlled and adjusted. The system also contains a CTD, transmissometer, dissolved oxygen sensor, precision pressure transducer, clinometer, compass, a video-microscope, and two additional video cameras for monitoring the flow direction and system performance.

WORK COMPLETED

PIV measurements were performed in June 6-20, 2003 at two locations while deploying the system from R/V Cape Hatteras. The first site is located in the vicinity of the R2 leg of SABSOON, at 31.336N; 80.694W, in water depth of 23m. The second site is located northeast from SABSOON, 32.226N; 79.95W, at a depth of 22m. The horizontal separation between the two sample areas of 35x35 cm was 66cm, enabling measurements of turbulence structures up to scales of 110 cm. The data was collected in different phases of a strong tidal current and at varying elevations above the bottom Overall 1.3 TB of PIV images were collected. Data analysis is presently in progress.

Figure 1 presents samples of mean horizontal velocity distributions of the first run, recorded on the night of June 11¯12 during accelerating, peak, and decelerating phase of the tidal cycle, while traversing the boundary layer. At each elevation, 20 minutes runs at a sampling frequency of 3 Hz provides 3600 PIV images. The timing of each data set is indicated with respect to that of the tidal peak. Averaging of all the 63 vectors at the same elevation, implies that each line in Figure 1 represents 63x226800 data points. Once the analysis is completed, these data sets will enable us to examine the structure of turbulence in the same site at substantially different mean flows (Reynolds numbers), following procedures illustrated using older data in the next section.

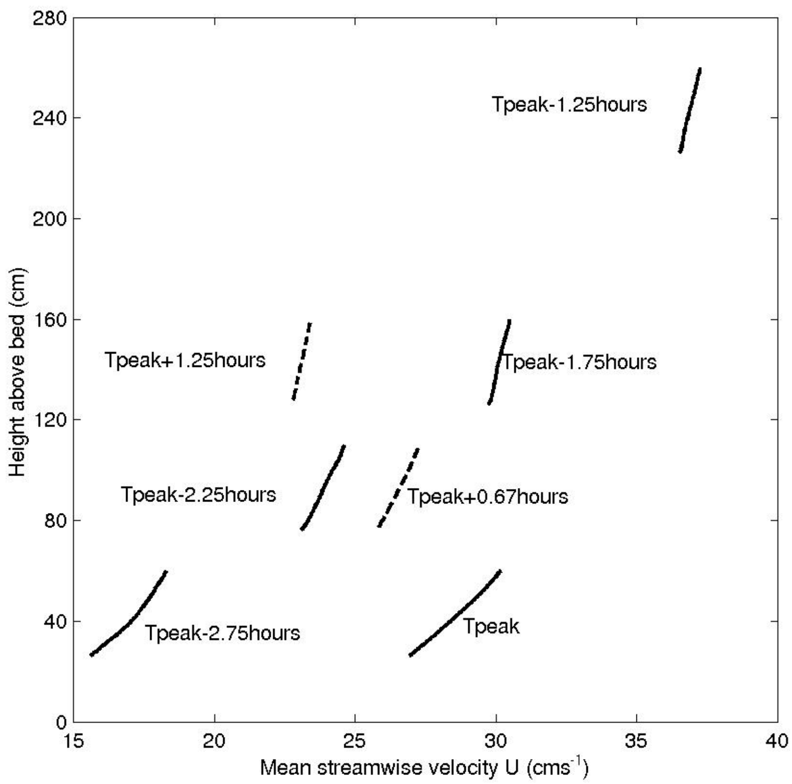

Figure 1: Mean horizontal velocity distributions obtained at different phases of a tidal cycle in the vicinity of SABSOON. T_{peak} represents the timing of peak tidal flow.

RESULTS

In this section we present sample results of data analysis performed on older data recorded in the vicinity of LEO-15. Further details and other data sets are available in reference 6. As noted before, the

PIV data demonstrates that the flow in the boundary layer at moderate speeds (10-20 cm/s mean velocity) consists of gusts with powerful vortical structures with periods of more quiescent flow between them. Figure 2 presents two characteristic instantaneous velocity and vorticity distributions of quiescent (left) and gust (right) periods. During a quiescent period there are no large-scale structure and the flow is dominated by very small (< 2cm diameter), weak eddies. During a gust period, groups of large (~10cm) vortices appear within the flow, either as isolated structures (as shown) or as elongated trains of eddies. In both cases, these structures are very coherent in both time and space, as one can observe by examining the time series, and by comparing data recorded by the two cameras.

Combining and examiming the data from a series of velocity distributions (not shown, see ref. 6) confirms that the coherent pattern of large separated vortices is consistent with a vertical section through a packet of hairpin vortices observed in laboratory studies (ref. 1). As the mean velocity increases, the periods between gusts decrease, eventually disappearing. In periods with no mean flow, but with wave-induced motion, the gusts disappear, and the velocity distributions resemble the quiescent sample shown in Figure 2.

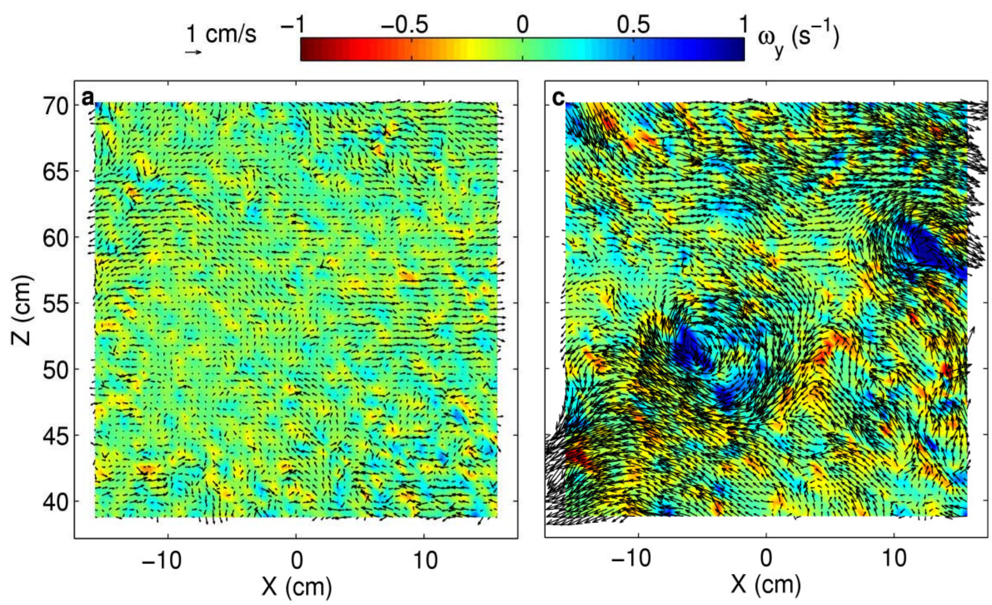

Figure 2: Characteristic instantaneous velocity (vectors) and vorticity (color) distributions during quiescent (left side) and gust (right side) periods.

In the previous report we presented several turbuelnt energy spectra obtained from the PIV data. Subsequently, we have performed conditional sampling of the data in order to compare the characteristics of turbulence in gusts and quiescent periods. The selection is based on the characteristic vorticity magnitude within each vector map. Sample comparisons of conditionally sampled spectra are presented in Figure 3.

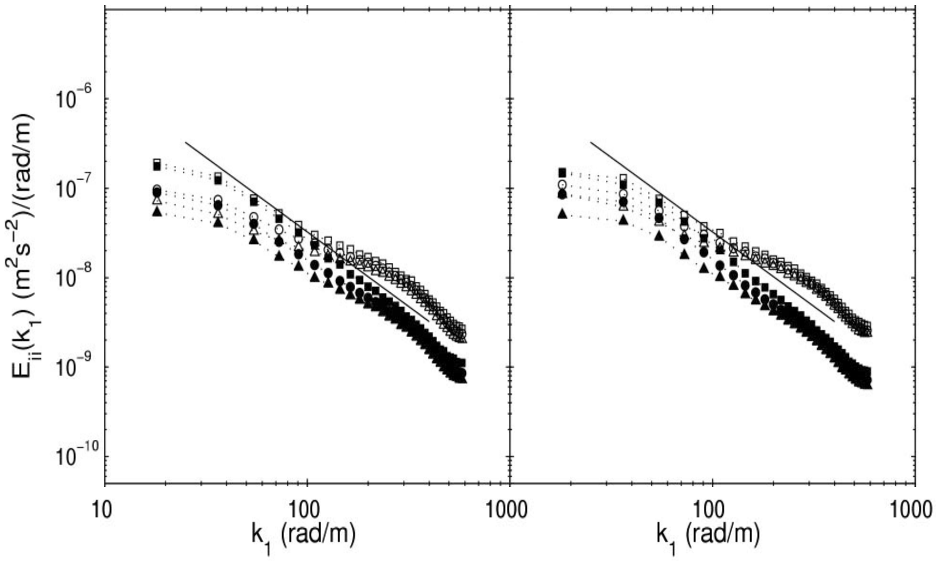

Figure 3: Mean spectra, conditionally sampled based on the vorticity magnitude. Left: depth of 257 cm; right: depth of 55 cm. Open symbols: $E_{11}(k_1)$; Closed symbols: $\frac{3}{4}E_{33}(k_1)$. Substcripts 1 and 3 represent the horizontal and vertical directions, respectively. Squares: high vorticity; Circles: intermediate vorticity; Triangles: low vorticity. The solid line has a slope of –5/3.

As is evident, the turbulence is nearly isotropic at low wavenumbers but becomes increasingly anisotropic with increasing wavenumber, the latter regardless of vorticity. This high-wavenumber anisotropy is most evident when the mean flow is weakest and the wave-induced oscillatory motion is dominant (ref. 6). At low wavenumbers the turbulence appears to be more isotropic during the high vorticity events, and more anisotropic during periods of low vorticity. In fact, most of the variability associated with vorticity magnitude occurs in the low-wavenumber ends of the spectra, consistent with the formation of intermittent, large-diameter vortices.

Interestingly, conditionally sampled dissipation rates (not shown here), being associated with the small-scale structures, do not vary substantially with vorticity magnitude. The background dissipation rate remains almost unchanged throughout the data series, irrespective of the presence of large-scale vortical structures. In stark contrasts to this finding are the conditionally sampled Reynolds shear stresses, estimated using the structure function, D_{13}, following the methodology described in refs 4 and 7. The distributions of $D_{13}(r)$, presented in Figure 4, demonstrate that the contributions to the stresses are made almost entirely by the high and intermediate vorticity magnitude events, while in the low vorticity regions the shear stresses are essentially zero. Thus, in times with weak mean flow but with wave orbital motion, the Reynolds stresses are very low. Conditional sampling based on phase in the wave orbital cycle does not show any significant trends.

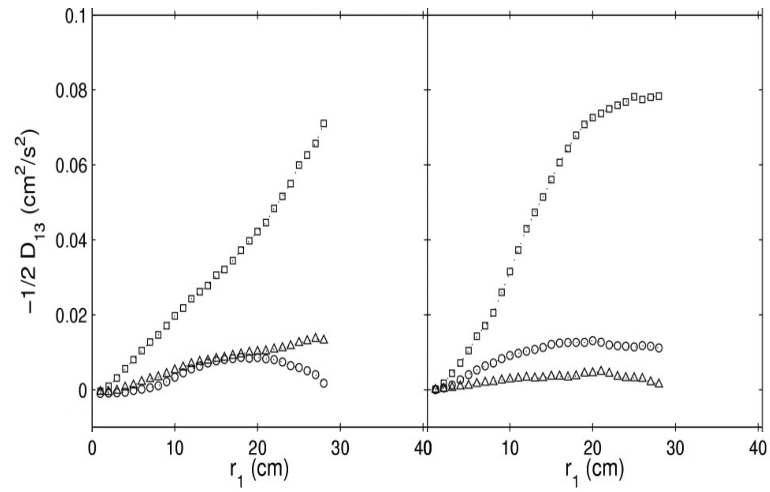

Figure 4: Sample conditionally sampled distributions of $-1/2D_{13}$ as a function of horizontal separation (r_1). Left: depth of 257 cm; right: depth of 55 cm. Squares: high vorticity; circles: intermediate vorticity; triangles: low vorticity.

Finally, in an attempt to understand the implications of the anisotropy demonstrated by the spectra, we compare the characteristic shapes of large and small scale turbulent structures. The data is spatially filtered using a box filter, and the resulting low-pass and high-pass vorticity distributions are presented in Figure 5. Clearly, the large scale structure has comparable horizontal and vertical scales (see also Figure 2), whereas the small scale structures appear to be elongated in the horizontal direction. Meandering of these small structures would cause higher fluctuations of the horizontal velocity component compared to the vertical component. The anisotropy at small scales is clearly evident.

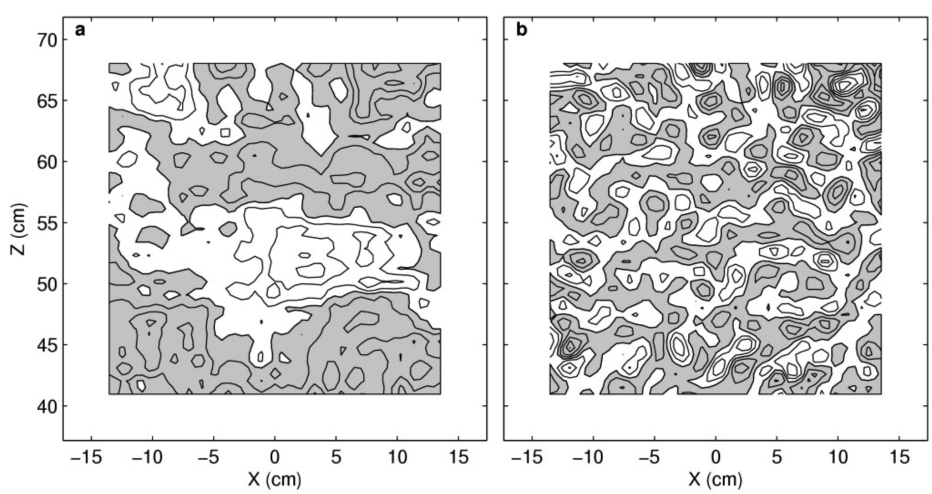

Figure 5: Sample instantaneous filtered vorticity using: a. A low-pass filter (k < 127 rad/m), contoured at intervals of 0.015s^{-1}; b. A band-pass filter (127 rad/m < k < 381 rad/m), contoured at intervals of 0.05s^{-1}. Negative values are shaded gray and the transition is the zero level.

IMPACT/APPLICATIONS

The present measurements and analysis enable us to characterize the flow structure and turbulence in the bottom boundary layer of the coastal ocean in great detail. The measurements provide distributions of Reynolds stresses, spectra, dissipation rate, characteristics of SGS stresses and energy transfer across scales, all free of contamination by surface waves. These data are essential for modeling of coastal circulation, sediment and pollutant transport, as well as biological processes.

TRANSITIONS

During FY 2000 & 2001 the present submersible PIV system has been used extensively at NSWC/Carderock to measure the flow structure within wakes behind several maneuvering models. Since then, graduates of our program that currently work at NSWC have constructed another system in order to handle the increasing demand. The present PIV system has also been deployed this year in a corn field to measure the structure of atmospheric turbulence and pollen transport.

RELATED PROJECTS

The research involving measurements of flow structure and turbulence in the coastal ocean using PIV has been funded in part by ONR (present project) and in part by NSF. The NSF sponsored project focuses with the flow/turbulence in the water column above the boundary layer, whereas the present project focuses on the boundary layer.

REFERENCES

1. Adrian, R.J., C.D. Meinhart, and C.D. Tomkins, 2000: Vortex organization in the outer region of the turbulent boundary layer. *J. Fluid Mech.*, **422**, 1-54.

2. Bertuccioli, L., G. I. Roth, J. Katz, and T. R. Osborn, 1999: A submersible Particle Image Velocimetry system for turbulence measurements in the bottom boundary layer. *J. Atmos. Oceanic Technol.*, **16,** 1635-1646.

3. Doron, P., L. L. Bertuccioli, J. Katz, and T. R. Osborn, 2001: Turbulence characteristics and dissipation estimates in the coastal ocean bottom boundary layer from PIV data. *J. Phys. Oceanogr.*, **31**, 2108-2134.

4. Nimmo Smith, W. A. M., P. Atsavapranee, J. Katz, and T. R. Osborn, 2002: PIV Measurements in the bottom boundary layer of the coastal ocean. *Exp. Fluids,* **33**, 962-971.

5. Nimmo Smith, W. A. M., J., Osborn, T.R., and J. Katz, 2003, PIV Measurements In The Bottom Boundary Layer Of The Coastal Ocean, chapter 4 in *PIV and Water Waves*, edited by P. L. F Liu, G. K. Pedersen and J. Grue, Publisher: World Scientific.

6. Nimmo Smith, W. A. M., J. Katz and T. R. Osborn, 2003: On the Structure of Turbulence in the Bottom Boundary Layer of the Coastal Ocean, *J. Phys. Oceanogr.*, submitted.

7. Trowbridge, J.H., 1998: On a technique for measurement of turbulent shear stress in the presence of surface waves*, J. Atmos. Oceanic Technol.*, **15**, 290-298.

PUBLICATIONS

1. Nimmo Smith, W. A. M., P. Atsavapranee, J. Katz, and T. R. Osborn, 2002: PIV Measurements in the bottom boundary layer of the coastal ocean. *Exp. Fluids,* **33**, 962-971. [published, refereed]

2. Nimmo Smith, W. A. M., J., Osborn, T.R., and J. Katz, 2002, PIV Measurements In The Bottom Boundary Layer Of The Coastal Ocean. [published]

3. Nimmo Smith, W. A. M., J., Osborn, T.R., and J. Katz, 2002, PIV Measurements In The Bottom Boundary Layer Of The Coastal Ocean, chapter 4 in *PIV and Water Waves*, edited by P. L. F Liu, G. K. Pedersen and J. Grue, Publisher: World Scientific. [in press, refereed]

4. Osborm T.R., Nimmo Smith, W.A.M., Luznik, L., Zhu, W., and J. Katz, 2002: Stress Calculations From PIV Measurements in The Bottom Boundary Layer, The 11th International Biennial Conference on Physics of Estuaries and Coastal Seas, Hamburg, Germany, September 17-20. [published]

5. Nimmo Smith, W. A. M., J. Katz and T. R. Osborn, 2003: On the Structure of Turbulence in the Bottom Boundary Layer of the Coastal Ocean, *J. Phys. Oceanogr.*, submitted.